Supermassive boson star at the galactic center?

Diego F. Torres*
Instituto Argentino de Radioastronomía, C.C.5, 1894 Villa Elisa, Buenos Aires, Argentina

S. Capozziello† and G. Lambiase‡
Dipartimento di Scienze Fisiche E.R. Caianiello, Università di Salerno, 84081 Baronissi (SA), Italy
and Istituto Nazionale di Fisica Nucleare, Sez. Napoli, Napoli, Italy
(Received 25 June 2000; published 13 October 2000)

We explore whether supermassive nonbaryonic stars (in particular boson, miniboson, and nontopological soliton stars) might be at the center of some galaxies, with special attention to the Milky Way. We analyze, from a dynamical point of view, what current observational data show, concluding that they are compatible with a single supermassive object without requiring it to be a black hole. Particularly, we show that scalar stars fit very well into these dynamical requirements. The parameters of different models of scalar stars necessary to reproduce the inferred central mass are derived, and the possible existence of boson particles with the adequate range of masses is commented upon. Accretion to boson stars is also briefly analyzed, and a comparison with another nonbaryonic candidate, a massive neutrino ball, which is also claimed as an alternative to the central black hole, is given. Both models are capable of explaining the nature of the object in Sgr A* without invoking the presence of a singularity. One difficult issue is why the accreted materials will not finally produce, in a sufficiently long time, a black hole. We provide an answer based on stellar disruption in the case of boson stars, and comment on several suggestions for its possible solution in neutrino ball scenarios. Finally, we discuss the prospects for the observational detection of these supermassive scalar objects, using the new generation of x-ray and radio interferometry satellites.

PACS number(s): 04.40.Dg, 98.35.Jk

I. INTRODUCTION

During recent years, ideas concerning the possible existence of a single large mass in the Galactic Center have been favored. This was a direct consequence of tightening the upper bound on its size, and the study of stability criteria, which ruled out complex clusters. Although it is commonly believed that this central mass is a supermassive black hole, it is not yet established, as we discuss below, on a firm observational basis.

The aim of this paper is to present an alternative model for the supermassive dark object in the center of our Galaxy, formed by self-gravitating nonbaryonic matter composed of bosons. These kinds of objects, so-called boson stars, are well known to physicists, but up to now, observational astrophysical consequences have hardly been explored. The main characteristics of this model are (1) it is highly relativistic, with a size comparable to (but slightly larger than) the Schwarzschild radius of a black hole of equal mass, (2) it has neither an event horizon nor a singularity, and after a physical radius is reached, the mass distribution exponentially decreases, and (3) the particles that form the object interact between each other only gravitationally, in such a way that there is no solid surface to which falling particles can collide.

It is the purpose of this work to show that these features are able to produce a Galactic Center model which can be confronted with known observational constraints, and to point to some of the ways in which such a center could be differentiated from a usual supermassive black hole.

Why scalar fields? Interesting models for dark matter use weakly interacting bosons (see, for instance, Refs. [1,2]).[1] Primordial nucleosynthesis shows that most of the mass in the universe should be nonbaryonic if $\Omega \sim 1$. Most models of inflation make use of scalar fields. Scalar-tensor gravitation is the most interesting alternative to general relativity. Recent results from supernovae, which in principle were thought of to favor a cosmological constant [3], can be supported by a variety of models as well, some of them with scalar fields too [4]. Particle physicists expect to detect the scalar Higgs particle in the next generation of accelerators. Scalar dilatons appear in low-energy unified theories, where the tensor field $g_{\mu\nu}$ of gravity is accompanied by one or several scalar fields, and in string effective supergravity. The axion is a scalar with a long history as a dark matter candidate, and Goldstone bosons also have already inferred masses. Symmetry arguments, which once led to the concept of neutron stars, may force to ask whether there could be stellar structures made up of bosons instead of fermions.

In recent works, Schunck and Liddle [5], Schunck and Torres [6], and Capozziello, Lambiase, and Torres [7] ana-

*Email address: dtorres@venus.fisica.unlp.edu.ar
†Email address: capozziello@sa.infn.it
‡Email address: lambiase@sa.infn.it

[1]In particular, the results of Ref. [1], which were obtained with a real scalar field, could equally well work with a complex scalar, such as the one that will be used here to introduce the boson star system. In this way, it is not discarded that the same scalar field could provide several solutions at the same price: for halos of galaxies, for the dark matter problem, and for the centers of some galaxies, as this work proposes.

lyzed some of the observational properties of boson stars. In particular, the Čerenkov effect, the gravitational redshift of the radiation emitted within a boson star potential, and the rotational curves of accreted particles were studied to assess possible boson star detection. These works extend previous ideas put forward by Tkachev [8]. The interest in observational properties of boson stars also led to the investigation of them as sources of γ-ray bursts [9] and as a possible lens in a gravitational lensing configuration [10]. Recent studies are analyzing the gravitational lensing phenomenon in strong field regimes [11–13]. This would be the case for boson stars, which are genuine relativistic objects.

This work is organized as follows. Section II is a brief summary of the main observational results concerning Sgr A*, and the main hypotheses in order to explain it are outlined there. Section III analyzes what dynamical observational data show, and what kind of models can support them. Section IV gives the basic ingredients to theoretically construct scalar stars, shows mass and radius estimates, and studies effective potentials and orbits of particles. In Sec. V we study the center of the Galaxy, show which are the stable scalar star models able to fit such a huge mass, and comment on the possible existence of boson particles with the required features. We also provide there an assessment of the disruption processes in boson star scenarios. Discussion and conclusions are given in Secs. VI and VII.

II. THE GALACTIC CENTER

A. Main observational facts

The Galactic Center is a very active region toward the Sagittarius constellation where, at least, six very energetic radio sources are present (Sgr A, A*, B1, B2, C, and D). There are several supernova remnants, filaments, and very rich star clusters. Several observational campaigns [14] have identified the exact center with the supermassive compact dark object in Sgr A*, an extremely loud radio source. The mass and the size of the object has been established to be $(2.61\pm0.76)\times10^6 M_\odot$ concentrated within a radius of 0.016 pc (about 30 lds) [15,16].

More precisely, Ghez *et al.* [15] have made extremely accurate velocity measurements in the central square arcsecs. From this bulk of data, it is possible to state that a supermassive compact dark object is present at the Galactic Center. It is revealed by the motion of stars moving within projected distances around 0.01 pc from the radio source Sgr A*, at projected velocities around 1000 $\mathrm{km\,s^{-1}}$. In other words, a high increase in the velocity dispersion of the stars toward the dynamical center is revealed. Furthermore, a large and coherent counter-rotation, especially of the early-type stars, is shown, supporting their origin in a well-defined epoch of star formation. Observations of stellar winds nearby Sgr A* give a mass accretion rate of $dM/dt=6\times10^{-6}M_\odot\ \mathrm{yr^{-1}}$ [16]. Hence, the dark mass must have a density $\sim10^9 M_\odot\ \mathrm{pc^{-3}}$ or greater, and a mass-to-luminosity ratio of at least $100M_\odot/L_\odot$. The bottom line is that the central dark mass seems to be a single object, and that it is statistically very significant ($\sim6-8\sigma$).

B. Domain of the black hole?

Such a large density contrast excludes that the dark mass could be a cluster of almost 2×10^6 neutron stars or white dwarfs. Detailed calculations of evaporation and collision mechanisms give maximal lifetimes of the order of 10^8 years, much shorter than the estimated age of the Galaxy [17,18].

As a first conclusion, several authors state that in the Galactic Center there is either a single supermassive black hole or a very compact cluster of stellar size black holes [16]. We shall come back to this paradigm through the rest of the paper (particularly in Sec. III).

Dynamical evidence for central dark objects has been published for 17 galaxies, such as M87 [19,20], or NGC4258 [21], but proofs that they really are black holes requires the measurement of relativistic velocities near the Schwarzschild radius, $r_s\simeq2M_\bullet/(10^8\ M_\odot)$ a.u. [22]. Because of the abovementioned mass accretion rate, if Sgr A* is a supermassive black hole, its luminosity should be more than $10^{40}\ \mathrm{erg\,s^{-1}}$, provided the radiative efficiency is about 10%. On the contrary, observations give a bolometric luminosity less than $10^{37}\ \mathrm{erg\,s^{-1}}$, already taking into account the luminosity extinction due to interstellar gas and dust. This discrepancy is the so-called ''blackness problem'' which has led to the notion of a ''black hole on starvation.'' Standard dynamics of the spherical accretion onto a black hole must be modified in order to obtain successful models (see, for instance, Ref. [23]). Recent observations, we recall, probe the gravitational potential at a radius larger than 4×10^4 Schwarzschild radii of a black hole of mass $2.6\times10^6 M_\odot$ [15].

C. Domain of the massive neutrino?

An alternative model for the supermassive compact object in the center of our Galaxy has been recently proposed by Tsiklauri and Viollier [24]. The main ingredient of the proposal is that the dark matter at the center of the galaxy is nonbaryonic (but in any case fermions, e.g., massive neutrinos or gravitinos), interacting gravitationally to form supermassive balls in which the degeneracy pressure balances their self-gravity. Such neutrino balls could have formed in early epochs, during a first-order gravitational phase transition, and their dynamics could be reconciled, with some adjustments, to the standard model of cosmology.

Several experiments are today running to search for neutrino oscillations. In order to explain the characteristics of Sgr A*, it would be necessary to have neutrinos with masses between 10 and 25 keV which, cosmologically, fall into the category of warm dark matter. It is interesting to note that the existence of gravitinos in this mass range allows for the formation of supermassive objects from $10^6 M_\odot$ to $10^9 M_\odot$.

One appealing characteristic of this model is that such a neutrino condensate could act as a spherical thick lens (a magnifying glass) for the stars behind it, so that their apparent velocities will be larger than in reality. In other words, depending on the line of sight, it should be possible to correct the projected velocities by a gravitational lensing contribution, so trying to explain the bimodal distribution (early

and late type stars) actually observed [15,16]. A detailed model and comparison with the data was presented by some of us [25].

III. OBSERVATIONAL STATUS

A. Brief review on dynamical data and what are they implying

An important information on the central objects of galaxies (particularly in active galactic nuclei) is the short time scale of variability. This has the significance of putting an upper bound—known as the causality constraint—on the size of the emitting region: If a system of size L suddenly increases its emissivity at all points, the temporal width with which we receive it is L/c and thus, a source cannot fluctuate in a way that involves its entire volume in time scales shorter than this (unless c is not a limiting velocity). This finally yields a corresponding maximum length scale, typically between 10^{-4} to 10 pc [26]. Autocorrelation in the emission argue against the existence of a cluster of objects (unless only one member dominates the emissivity), and the small region in which the cluster should be allows two body encounters to be very common and produces the lost of the stability of complex clusters. These facts can be used to conclude that a single massive object must be in the center of most galaxies. What observations show in this case is that the size of the emitting regions are very small. This does not directly implicate black holes as such.

The way in which we expect to detect the influence of a very massive object is through its gravity. The ''sphere of influence'' of a large mass is defined by the distance at which its potential significantly affects the orbital motions of stars and gas, and is given by

$$R_* = GM/\sigma_*^2 \sim 4 M_7 \sigma_{*,100}^{-2} \ \text{pc}, \tag{1}$$

where the central mass is normalized to $10^7 M_\odot$ and $\sigma_{*,100}$ is a r.m.s. orbital speed in units of 100 km s^{-1}. Thus, even very large masses have a small sphere of influence. Within this sphere, the expected response to a large nuclear mass can be divided in two groups. First, the response of interstellar gas can hardly be anything different from an isotropic motion in the center of mass frame. Random speeds are often thought to be much smaller than this overall speed, which far from the sphere of influence is just given by $(GM/r)^{1/2}$. If the energy produced by random motions is radiated away, the gas behaves as a whole and tends to flatten itself, conserving the angular momentum. Observations of the rotational velocity of gas as a function of the radius can thus provide a measure of the total mass at the center. Then, what observation searches is the existence of a Keplerian potential signature in the flattened gas velocity distribution. Examples of this are the radio galaxies M87 [19], NGC 4258 [27], and many others. Then, any massive object producing a velocity distribution with a Keplerian decrease would be allowed by observation.

Secondly, we consider the response of the stars. In this case, peculiar velocities are larger or comparable to the bulk streaming and it is harder to actually differentiate the stellar response to a nuclear mass from the observable properties of a pure stellar potential. However, stellar motions, contrary to that of gas, are not affected by other forces (such as those produced by magnetic fields), and are better tracers of mass distributions. What observations show in this case are the stellar density and the velocity distribution. Use of the collisionless Boltzmann equation allows one to get the Jean's relation [28,26]

$$\frac{GM(r)}{r} = V_{\text{rot}}^2 - \sigma_r^2 \left[\frac{d \ln n(r)}{d \ln r} - \frac{d \ln \sigma_r^2}{d \ln r} + 2 - \frac{\sigma_t^2}{\sigma_r^2} \right]. \tag{2}$$

Here, $n(r)$ is the spherically symmetric distribution of stars, V_{rot} is the mean rotational speed, $\sigma_{r,\theta,\phi}$ are velocity dispersions, and $\sigma_t^2 = \sigma_\theta^2 + \sigma_\phi^2$. Measurements of V and random velocities determine that $M(r)$ decline inwards until a critical radius, where—as long as the resolution is available—M becomes constant. What really happens, however, is that even if this region is not scrutinized, the mass to light ratio becomes sufficiently large to suggest the presence of a large dark mass. A combination of this with other measurements strongly suggest that this dark mass is a single object. The black hole scenario has become our paradigm. But suggestions that the dark objects are black holes are based only on indirect astrophysical arguments, and surprises are possible on the way to the center [22].

B. The galaxy

We follow Genzel *et al.* [16] and parametrize the stellar density distribution as

$$n(r) = \frac{\Sigma_0}{R_0} \frac{1}{1 + (R/R_0)^\alpha}. \tag{3}$$

Note that R_0 is related to the core radius through $R_{\text{core}} = b(\alpha) R_0$. Genzel *et al.* found that the best fit parameters for the observed stellar cluster are a central density of $4 \times 10^6 M_\odot \ \text{pc}^{-3}$, a core radius of 0.38 pc, and a value $\alpha = 1.8$ [$b(\alpha) = 2.19$]. With this distribution, they found that a dark mass of about $2.5 \times 10^6 M_\odot$ was needed to fit the observational data.

The cluster distribution, and the cluster plus a black hole constant mass is shown in Fig. 1. Black boxes represent Genzel *et al.* (Table 10) and Eckart and Genzel (Fig. 5) data. A dashed line stands for the stellar cluster contribution, while a dot-dashed line represents an enclosed pointlike black hole mass. The solid line in the right half of the figure stands for the mass distribution both for a black hole and a boson star plus the stellar cluster. The mass dependence we are plotting for the boson star is obtained in Sec. IV, and represents the mass distribution of a miniboson star ($\Lambda = 0$, $m[\text{GeV}] = 2.81 \times 10^{-26}$) with dimensionless central density $\sigma(0)$ equal to 0.1. Other boson star configurations, with an appropriate choice of the boson field mass m, yield the same results. Note the break of more than three orders of magnitude in the x axis. This is caused because the boson star distribution, further out of the equivalent Schwarzschild radius, dynamically behaves as a black hole. It begins to differ from

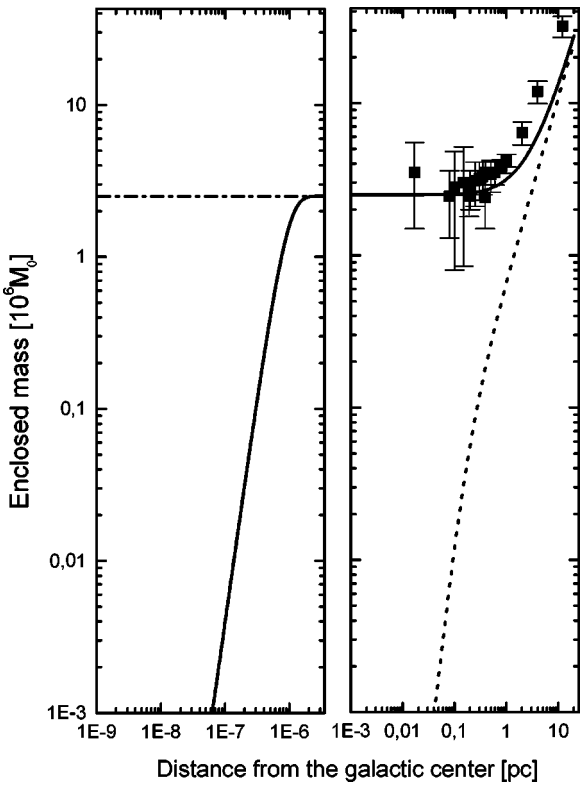

FIG. 1. Enclosed mass in the center of the galaxy together with observational data points. See discussion in the main text.

the black hole case at radius more than three orders of magnitude smaller than at that we have the innermost data point. From the mass distribution, a boson star in the center of the galaxy is virtually indistinguishable from a black hole.

Tsiklauri and Viollier [24] have shown that the same observational data can also be fitted using an extended neutrino ball. In that case, differences begin to be noticed just around the innermost data point. It is then hard to determine whether the central object is a black hole, a neutrino ball, or a boson star based *only* on dynamical data now at hand, and other problems concerning the accretion disk have to considered (see below). Even harder is the situation for deciding—using only this kind of data—if the supermassive object is a boson star instead of a black hole: as a boson star is a relativistic object, the decay of the enclosed mass curve happens close to the center. This, however, will provide an equivalent picture than a black hole for disruption and accretion processes; we shall comment on it in the next sections.

To apply Eq. (2) to the observational data we have to convert intrinsic velocity dispersions $[\sigma_r(r)]$ and volume densities $[n(r)]$ to projected ones [28], these are the ones we observe. We shall also consider that $\delta=1-\sigma_\theta^2/\sigma_r^2$, the anisotropy parameter, is equal to 0, and we are assuming implicitly that $\sigma_\theta=\sigma_\phi$. We take into account the following Abel integrals:

$$\Sigma(p)=2\int_p^\infty \frac{n(r)r}{\sqrt{r^2-p^2}}dr, \tag{4}$$

$$\Sigma(p)\sigma_r(p)=2\int_p^\infty \frac{n(r)\sigma_r(r)^2 r}{\sqrt{r^2-p^2}}dr. \tag{5}$$

$\Sigma(p)$ denotes surface density, $\sigma_r(p)$ is the projected velocity dispersion, and p is the projected distance. We adopt the Genzel *et al.* [16] parametrization for $\sigma_r(r)$,

$$\sigma_r(r)=\sigma(\infty)^2+\sigma(2'')^2\left(\frac{R}{2''}\right)^{-2\beta}. \tag{6}$$

What one usually does is to numerically integrate Eqs. (4), (5) and fit the observational data [$\sigma_r(p)$ vs p]. To do so one also has to assume a density dependence for the cluster [as in Eq. (3)], and the dark mass. With a pointlike dark mass of $2.5\times10^6 M_\odot$, the parameters of the fit result to be $\sigma(\infty)=55\ \mathrm{km\,s^{-1}}$, $\sigma(2'')=350\ \mathrm{km\,s^{-1}}$, and $\beta=0.95$.

If one now changes the central black hole for a boson star, one has to consider its particular density dependence. In this way, $n(r)=n_{\text{stellar cluster}}(r)+n_{\text{dark mass}}(r)$. We obtained $n_{\text{boson star}}(r)$ as $M(r)/(4/3\pi r^3)$, where $M(r)$ is the fitted mass dependence of the boson star as explained in the next section. It is now useful to consider that the fitting of $\sigma_r(p)$ is made taking into account observational data points in regions where the boson star generated space-time is practically indistinguishable from a black hole. Then, we may expect that the actual parameters $\sigma(\infty)$, $\sigma(2'')$, and β for $\sigma_r(r)$, will be very close to those obtained for the black hole. For our purposes, it is enough to take the same $\sigma_r(r)$ as in the black hole case, and compute $\sigma_{r\ \text{boson star}}(p)$ using Eqs. (4),(5), with the adequate total $n(r)$.

In Fig. 2 we show the observational data of Eckart and Genzel (filled black boxes) and Genzel *et al.* (hollow circles) superimposed with the curve for $\sigma_r(p)$ that we obtain with a miniboson star [$\Lambda=0$, $\sigma(0)=0.1$, $m[\mathrm{GeV}]=2.81\times10^{-26}$] in the galactic center. Other boson star configurations, with appropriate choice of the boson field mass m, yield to the same results. For this configuration, we used, as will be explained in Sec. IV, a mass distribution given by a Boltzmann-like equation with $A_2=2.5\times10^6 M_\odot$, $A_1=-0.237\times10^6 M_\odot$, $R_0=1.19210^{-6}$ pc, and $\Delta R=4.16310^{-6}$ pc. In the range plotted, and in which data is available, the differences between boson and black hole theoretical curves is undetectable. They only begin to deviate from each other at $p\sim10^{-4}$ pc. Even the deviation in such a region is as slight as $1\ \mathrm{km\,s^{-1}}$, and it only becomes more pronounced when p values are closer to the center. However, we should recall that it has no sense to go to such extreme values of p: the stars will be disrupted by tidal forces (see the discussion in Sec. VI) in those regions. Now we shall work out in detail the boson star model that we use.

IV. BOSON STARS

A. Basic concepts and configurations

Let us study the Lagrangian density of a massive complex self-gravitating scalar field (taking $\hbar=c=1$),

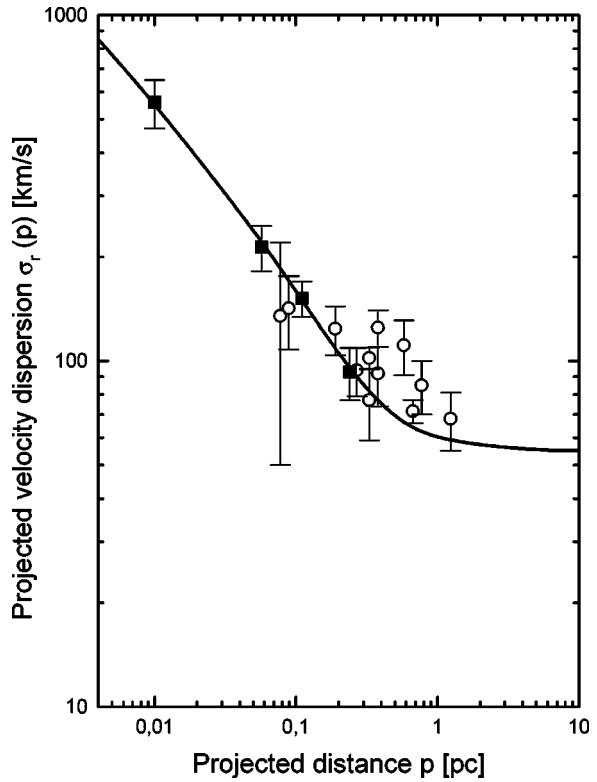

FIG. 2. Projected velocity dispersions: observational data and fit using a boson star model. See discussion in the main text.

$$\mathcal{L}=\frac{1}{2}\sqrt{|g|}\left[\frac{m_{\mathrm{Pl}}^2}{8\pi}R+\partial_\mu\psi^*\partial^\mu\psi-U(|\psi|^2)\right], \tag{7}$$

where R is the scalar of curvature, $|g|$ the modulus of the determinant of the metric $g_{\mu\nu}$, and ψ is a complex scalar field with potential U. Using this Lagrangian as the matter sector of the theory, we get the standard field equations

$$R_{\mu\nu}-\frac{1}{2}g_{\mu\nu}R=-\frac{8\pi}{m_{\mathrm{Pl}}^2}T_{\mu\nu}(\psi), \tag{8}$$

$$\Box\psi+\frac{dU}{d|\psi|^2}\psi=0, \tag{9}$$

where the stress energy tensor is given by

$$T_{\mu\nu}=\tfrac{1}{2}[(\partial_\mu\psi^*)(\partial_\nu\psi)+(\partial_\mu\psi)(\partial_\nu\psi^*)] -\tfrac{1}{2}g_{\mu\nu}[g^{\alpha\beta}(\partial_\alpha\psi^*)(\partial_\beta\psi)-U(|\psi|^2)] \tag{10}$$

and

$$\Box=\partial_\mu[\sqrt{|g|}g^{\mu\nu}\partial_\nu]/\sqrt{|g|} \tag{11}$$

is the covariant d'Alembertian. Because of the fact that the potential is a function of the square of the modulus of the field, we obtain a global $U(1)$ symmetry. This symmetry, as we shall later discuss, is related with the conserved number of particles. The particular form of the potential is what makes the difference between miniboson, boson, and soliton stars. Conventionally, when the potential is given by

$$U=m^2|\psi|^2+\frac{\lambda}{2}|\psi|^4, \tag{12}$$

where m is the scalar mass and λ a dimensionless constant measuring the self-interaction strength, miniboson stars are those spherically symmetric equilibrium configurations with $\lambda=0$. Boson stars, on the contrary, have a non-null value of λ. The previous potential with $\lambda\neq0$ was introduced by Colpi *et al.* [29], who numerically found that the masses and radius of the configurations were deeply enlarged in comparison to the miniboson case.

Soliton (also called nontopological soliton) stars are different in the sense that, apart from the requirement that the Lagrangian must be invariant under a global $U(1)$ transformation, it is required that—in the absence of gravity—the theory must have nontopological solutions; i.e., solutions with a finite mass, confined to a finite region of space, and nondispersive. An example of this kind of potentials is the one introduced by Lee and his co-workers [30]

$$U=m^2|\psi|^2\left(1-\frac{|\psi|^2}{\Phi_0^2}\right)^2, \tag{13}$$

where Φ_0 is a constant. In general, boson stars accomplish the requirement of invariance under a $U(1)$ global transformation but not the *solitonic* second requirement. To satisfy it, it is necessary that the potential contains attractive terms. This is why the coefficient of $(\psi^*\psi)^2$ of the Lee form has a negative sign. Finally, when $|\psi|\to\infty$, U must be positive, which leads, minimally, to a sixth order function of ψ for the self-interaction. It is usually assumed, because of the range of masses and radius for soliton stars in equilibrium, that they are huge and heavy objects, although this finally depends on the choice of the different parameters.

We shall now briefly explain how these configurations can be obtained [31–33]. We adopt a spherically symmetric line element

$$ds^2=e^{\nu(r)}dt^2-e^{\mu(r)}dr^2-r^2(d\vartheta^2+\sin^2\vartheta d\varphi^2), \tag{14}$$

with a scalar field time-dependence ansatz consistent with this metric:

$$\psi(r,t)=\sigma(r)e^{-i\omega t} \tag{15}$$

where ω is the (eigen)frequency. This form of the field—when it has no nodes—ensures us to be working in the configurations of minimal energy [30].

The nonvanishing components of the energy-momentum tensor are

$$T_0{}^0=\rho=\tfrac{1}{2}[\omega^2\sigma^2(r)e^{-\nu}+\sigma'^2(r)e^{-\mu}+U], \tag{16}$$

$$T_1{}^1=p_r=\tfrac{1}{2}[\omega^2\sigma^2(r)e^{-\nu}+\sigma'^2(r)e^{-\mu}-U], \tag{17}$$

$$T_2{}^2=T_3{}^3=p_\perp=-\tfrac{1}{2}[\omega^2\sigma^2(r)e^{-\nu}-\sigma'^2(r)e^{-\mu}-U], \tag{18}$$

where $'=d/dr$. The nonvanishing independent components of the Einstein equation are

$$\nu'+\mu'=\frac{8\pi}{m_{\rm Pl}^2}(\rho+p_r)re^{\mu}, \tag{19}$$

$$\mu'=\frac{8\pi}{m_{\rm Pl}^2}\rho re^{\mu}-\frac{1}{r}(e^{\mu}-1). \tag{20}$$

Finally, the scalar field equation is

$$\sigma''+\left(\frac{\nu'-\mu'}{2}+\frac{2}{r}\right)\sigma'+e^{\mu-\nu}\omega^2\sigma-e^{\mu}\frac{dU}{d\sigma^2}\sigma=0. \tag{21}$$

To do numerical computations and order of magnitude estimates, it is useful to have a new set of dimensionless variables. We adopt here

$$x=mr, \tag{22}$$

for the radial distance, we redefine the radial part of the boson field as

$$\sigma=\sqrt{4\pi}\sigma/m_{\rm Pl} \tag{23}$$

and introduce

$$\Lambda=\lambda m_{\rm Pl}^2/4\pi m^2, \quad \Omega=\frac{\omega}{m}. \tag{24}$$

In order to obtain solutions which are regular at the origin, we must impose the following boundary conditions $\sigma'(0)=0$ and $\mu(0)=0$. These solutions have two fundamental parameters: the self-interaction and the central density (represented by the value of the scalar field at the center of the star). The mass of the scalar field fixes the scale of the problem. Boundary conditions representing asymptotic flatness must be applied upon the metric potentials, these determine—which is actually accomplished via a numerical shooting method—the initial value of $\nu=\nu(0)$. Then, having defined the value of the self-interaction, or alternatively, the form of the soliton potential, the equilibrium configurations are parametrized by the central value of the boson field. As this central value increases, so does the mass and radius of the star. This happens until a maximum value is reached in which the star loses its stability and disperses away. Up to this value of σ_0, catastrophe theory can be used to show that these equilibrium configurations are stable [34]. As an example of boson star configurations, we show in Fig. 3, the mass and number of particles (see below) for a $\Lambda=10$ Colpi *et al.* potential, and in Fig. 4, the stability analysis.

When $\Lambda\gg 1$, we must follow an alternative adimensionalization [29]. For large Λ, we shift to the following set of variables:

$$\sigma_*=\sigma\Lambda^{1/2}, \tag{25}$$

$$x_*=x\Lambda^{-1/2}, \tag{26}$$

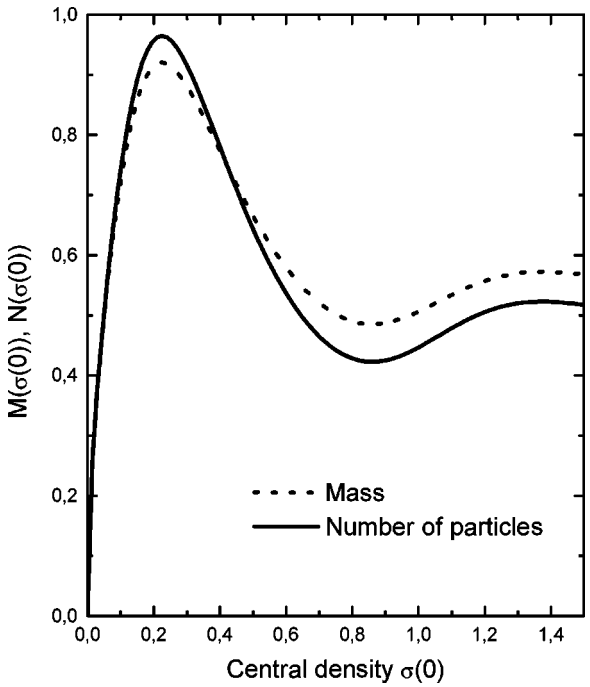

FIG. 3. Mass and number of particles, in dimensionless units, for a $\Lambda=10$ boson star (Colpi *et al.* [29]) potential.

$$M_*=M\Lambda^{-1/2}. \tag{27}$$

Here, M_* is defined by

$$e^{\mu}=\left(1-2\frac{M_*}{x_*}\right)^{-1}, \tag{28}$$

which corresponds to the Schwarzschild mass (see below). Ignoring terms $\mathcal{O}(\Lambda^{-1})$, the scalar wave equation is solved algebraically to yield

$$\sigma_*=(\Omega^2e^{-\nu}-1)^{1/2}, \tag{29}$$

and up to the same accuracy, the field equations are

$$\frac{dM_*}{dx_*}=\frac{1}{4}x_*^2(3\Omega^2e^{-\nu}+1)(\Omega^2e^{-\nu}-1), \tag{30}$$

$$\frac{d\nu}{dx_*}\frac{e^{-\mu}}{x_*}-\frac{1^2}{x^*}(1-e^{-\mu})=\frac{1}{2}(\Omega^2e^{-\nu}-1)^2. \tag{31}$$

The system now depends only on one free parameter $\Omega^2e^{-\nu(0)}$. Numerical solutions show that the maximum mass corresponding to a stable star is given by $M_{\rm max}\sim 0.22\Lambda^{1/2}m_{\rm Pl}^2/m$.

B. Masses estimates

The invariance of the Lagrangian density under a global phase transformation $\psi\rightarrow\psi e^{-i\vartheta}$ of the complex scalar field gives (via the Noether's theorem) a locally conserved current $\partial_\mu j^\mu=0$, and a conserved charge (number of particles). We need to study the number of particles because it is essential to determine whether the configurations are stable or not. A

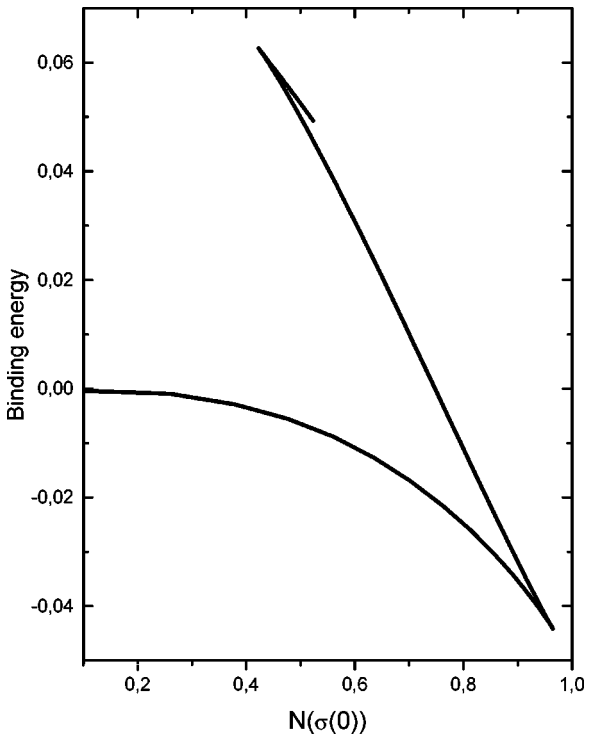

FIG. 4. Stability analysis for $\Lambda=10$ configurations. Catastrophe theory ensures that the first branch, which includes the (0,0) point, is the only stable one.

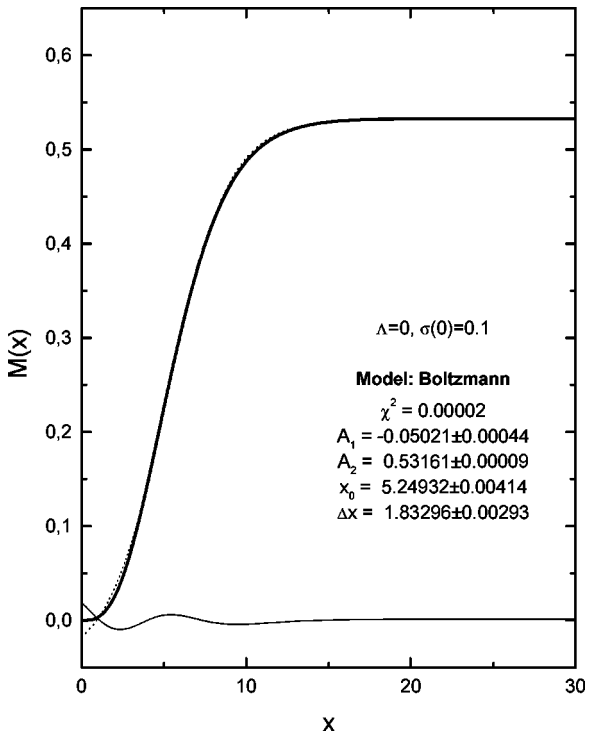

FIG. 5. Boson star mass as a function of x, for a $\Lambda=0$, $\sigma(0)=0.1$ model. We show a Boltzmann-like fitting, see text (dotted curve, but almost everywhere on the solid curve) and its residue (solid lower line).

necessary requirement towards the stability of the configurations is a negative binding energy ($BE=M-mN$), i.e., the star must be energetically more favorable than a group of unbound particles of equal mass. From the Noether theorem, the current j^μ is given by

$$j^\mu=\frac{i}{2}\sqrt{|g|}g^{\mu\nu}[\psi^*\partial_\nu\psi-\psi\partial_\nu\psi^*] \tag{32}$$

and the number of particles is

$$N:=\int j^0\,d^3x. \tag{33}$$

For the total gravitational mass of localized solutions, we may use Tolman's expression [35], or equivalently, the Schwarzschild mass

$$M=\int (2T_0^0-T_\mu^\mu)\sqrt{|g|}d^3x. \tag{34}$$

In Fig. 5, we show the mass of a boson star with $\Lambda=0$ as a function of x. We have fitted this curve with a Boltzmann-like function

$$M_{\rm fit}(x)=A_2+\frac{A_1-A_2}{1+e^{(x-x_0)/\Delta x}}, \tag{35}$$

which is reliable except in regions very near the center, where $M_{\rm fit}(x)$ becomes slightly negative. The χ^2 parameter of the fitting is around 10^{-5}, and values for A_1, A_2, and Δx are given in the figure. It is this formula that we have used in Fig. 2 to analytically get the $\sigma_r(p)$ dependence of the boson star (in the range we use the approximation, the actual mass and the fitting differ negligibly). Note also what the fitting is physically telling us: it represents a black hole of mass A_1 plus an inner exponentially decreasing correction. As far as we are aware, this is the first time that such a Boltzmann-like fitting has been done, and we think it could be usefully applied in other analytical computations. Models with different Λ and σ can be equally well fitted.

Since boson stars are prevented from gravitational collapse by the Heisenberg uncertainty principle, we may make some straightforward mass estimates [33]: For a boson to be confined within the star of radius R_0, the Compton wavelength has to satisfy $\lambda_\psi=(2\pi\hbar/mc)\leqslant 2R_0$. In addition, the star radius must be of the order of the last stable Kepler orbit $3R_S$ around a black hole of Schwarzschild radius $R_S:=2GM$. In the case of a miniboson star of effective radius $R_0\cong(\pi/2)^2R_S$ close to its Schwarzschild radius one obtains the estimate

$$M_{\rm crit}\cong(2/\pi)m_{\rm Pl}^2/m\geqslant 0.633M_{\rm Pl}^2/m. \tag{36}$$

The exact value in the second expression was found only numerically.

For a mass of $m=30$ GeV, one can estimate the total mass of this miniboson star to be $M\simeq 10^{10}$ kg and its radius $R_0\simeq 10^{-17}$ m, amounting a density 10^{48} times that of a neutron star. In the case of a boson star ($\lambda\neq 0$), since $|\psi|\sim m_{\rm Pl}/\sqrt{8\pi}$ inside the boson star [29], the energy density is

$$\rho \simeq m^2 m_{\rm Pl}^2 (1+\Lambda/8). \tag{37}$$

Equivalently, we may think that this corresponds to a star formed from noninteracting bosons with rescaled mass $m \to m/\sqrt{1+\Lambda/8}$ and consequently, the maximal mass scales with the coupling constant Λ as

$$M_{\rm crit} \simeq \frac{2}{\pi}\sqrt{1+\Lambda/8}\,\frac{m_{\rm Pl}^2}{m}. \tag{38}$$

There is a large range of values of mass and radius that can be covered by a boson star, for different values of Λ and σ_0. For instance, if m is of the order of the proton mass and $\lambda \simeq 1$, this is in the range of the Chandrasekhar limiting mass $M_{\rm Ch} := M_{\rm Pl}^3/m^2 \simeq 1.5 M_\odot$.

Larger than these estimates is the range of masses that a nontopological soliton star produces, this is because the power law dependence on the Planck mass is even higher: $\sim 10^{-2}(m_{\rm Pl}^4/m\Phi_0^2)$. These configurations are static and stable with respect to radial perturbations. It is by no means true, however, that these are the only stable equilibrium configurations that one can form with scalar fields. Many extensions of this formalism can be found. It is even possible to see that boson stars are a useful setting to study gravitation theory in itself [36]. Most importantly for our hypothesis is that rotating stable relativistic boson stars can also be found with masses and radii comparable in magnitude to their static counterparts [37]. In astrophysical settings it is usual to expect some induced rotation of stellar objects, and it is important that these rotations may not destabilize the structure. Another interesting generalization is that of electrically charged boson stars [38]. Although it is usually assumed that selective accretion will quickly discharge any astrophysical object, some recent results by Punsly suggest this may not always be the case [39].

C. Effective potentials

The motion of test particles can be obtained from the Euler-Lagrange equations taking into account the conserved canonical momenta [40]. In a general spherically symmetric potential, the invariant magnitude squared of the four velocity ($u^2 \equiv g_{\mu\nu}\dot{x}^\mu \dot{x}^\nu$), which is 1 for particles with nonzero rest mass and 0 for massless particles, yields

$$\dot{r}^2 = \frac{1}{g_{rr}}\left[\frac{E_\infty^2}{g_{tt}} - u^2 - \frac{l^2}{g_{\phi\phi}}\right], \tag{39}$$

where l and E_∞ are constants of motion given by $-g_{\phi\phi}\sin^2\theta\dot{\phi}$ and $g_{tt}\dot{t}$ (angular momentum and energy at infinity, both per unit mass), respectively, and an overdot stands for derivation with respect to an affine parameter. This equation can be transformed to

$$\tfrac{1}{2}\dot{r}^2 + V_{\rm eff} = \tfrac{1}{2}E_\infty^2 e^{-\mu-\nu}, \tag{40}$$

where $V_{\rm eff}$ is an effective potential. This name comes from the fact that in the Schwarzschild solution $e^{-\mu-\nu} \equiv 1$ and thus, the previous equation can be understood as a classical trajectory of a particle of energy $E_\infty^2/2$ moving in a central potential. This is not so in a more general spherically symmetric case, such as these nonbaryonic stars. In the boson star case, for instance, typical metric potentials are shown in Fig. 6; note that for them $e^{-\mu-\nu} \neq 1$. We can see, however, that $e^{-\mu-\nu} < e^{-\mu(0)-\nu(0)} = C$, where C is a constant, and then, usual classical trajectories can be looked at, in the sense that we may construct an equation of the form $\dot{r}^2/2 + V_{\rm eff} < 1/2E_\infty^2 e^{-\mu(0)-\nu(0)}$, and it will always be satisfied.

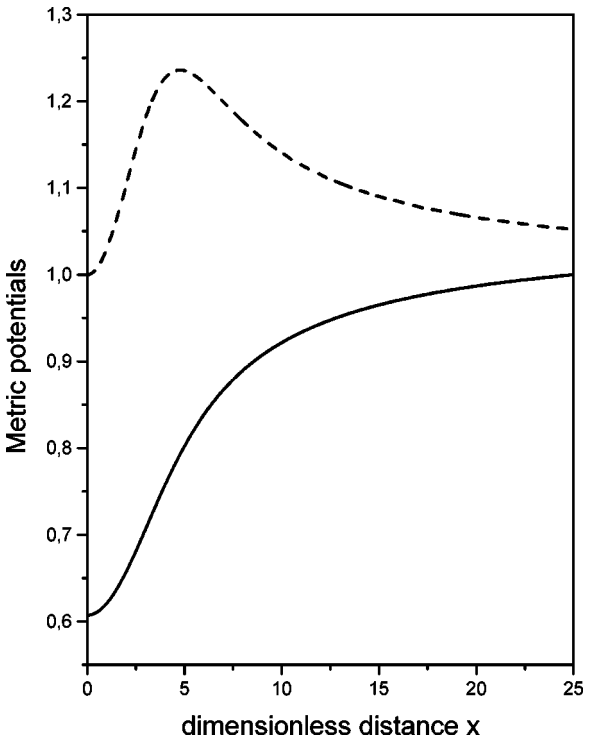

FIG. 6. Boson star metric potentials $g_{rr} = e^{\mu}$ (dashed) and $g_{tt} = e^{\nu}$ (solid). Boson star parameters are $\Lambda = 0$, $\sigma(0) = 0.1$, but the behavior is generic.

The effective potential that massive or massless particles feel must be very different from the black hole case. In the case of a massless particle, the effective potential is given by

$$V_{\rm eff} = e^{-\mu}\frac{l^2}{2r^2}, \tag{41}$$

while for a massive test particle it is

$$V_{\rm eff} = \frac{1}{2}e^{-\mu}\left(1 + \frac{l^2}{r^2}\right). \tag{42}$$

We show both boson (for the case of $\Lambda = 0$) and black hole potentials in Figs. 7 and 8. The mass of the central object is fixed to be the same in both cases (see captions) and the curves represent a fourth order Runge-Kutta numerical integration of the equations we previously derived with $\Lambda = 0$ and $\sigma(0) = 0.1$. In the case of massive test particles we use $l^2/M^2 = 0$, 12, and 15; thus explicitly showing the change in the behavior of $V_{\rm eff}$ for the black hole case. As l increases,

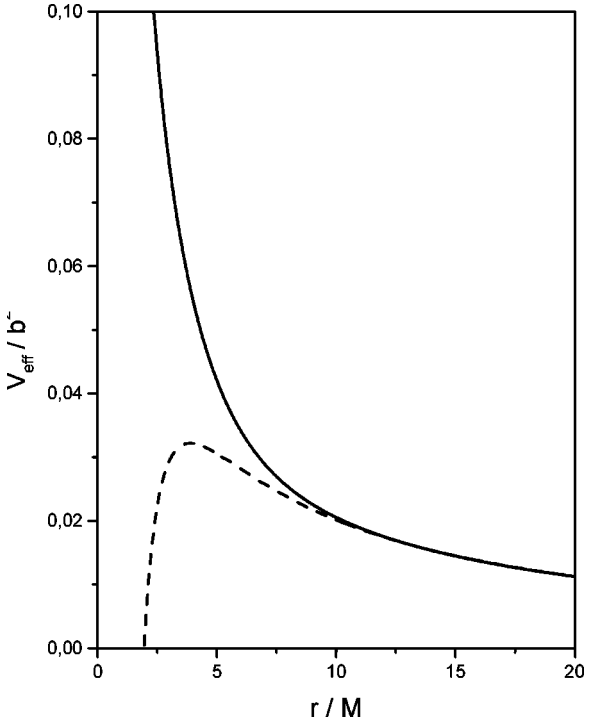

FIG. 7. Boson (solid) and Schwarzschild (dashed) effective potentials for massless particles $b=l^2/E_\infty^2$. The mass for both, the black hole and the boson star, was taken as $M=0.62089m_{\rm Pl}^2/m$. The maximum in the black hole case happens, independently of l, for $r/M=3$.

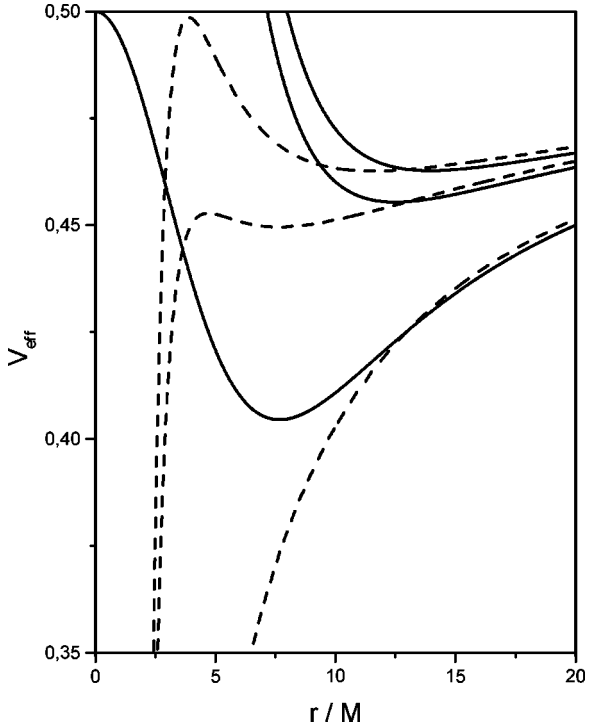

FIG. 8. Boson (solid) and Schwarzschild (dashed) effective potentials in the case of massive particles. The mass of the central object is as in the previous figure. The three curves correspond to $l^2/M^2=0$, 12, and 15 (from bottom to top).

this shape changes from a monotonous rising curve to one that has a maximum and a minimum before reaching its asymptotic limit. These extrema disappear for $l^2/M^2<12$. In the case of boson stars, however, if $l\neq 0$ we have a divergence in the center at $r=0$ and only one extremum—a minimum—which occurs at rising values of r/M as l grows. The curve $V_{\rm eff}$ for $l=0$—radially moving objects—is not divergent, and we can see that the particles may reach the center of the star with a non-null velocity, given by $1/2\dot{r}^2=1/2E_\infty^2 e^{-\mu(0)-\nu(0)}-V_{\rm eff}(0)>0$, and will then traverse the star unaffected.

For massless particles, the differences are also notorious: a black hole produces a negative divergence and a boson star a positive one. Radial motion of massless particles is insensitive to $V_{\rm eff}$, being this equal to zero, as in the Schwarzschild case. In both cases, for massive and massless particles, outside the boson star the potential mimics the Schwarzschild one.

D. Particle orbits

In the case of a black hole, orbits can be of three types: if the energy is bigger than the effective potential at all points, particles are captured. If the energy is such that the energy equals the effective potential just once, particles describe an unbound orbit, and the point of equality is known as turning point. If there are two such points, orbits are bound around the black hole. Orbits in which the energy equals the potential in a minimum of the latter are circular and stable ($\dot{r}=0$, $V''_{\rm eff}<0$).

We cannot, because of the different relationship between the metric potentials we commented above, do the same analysis using $V_{\rm eff}$ for the boson star. We can, however, note that in most cases the total equation for the derivative of r will be modified in a trivial way: If we look at the cases where the effective potential has a divergence at the center (and because the metric coefficients do not diverge), there is no other possibility for the particles more than to find a turning point. Orbits can then be bound or unbound depending on the energy, but we can always find a place where $\dot{r}=0$ and then it has to reverse its sign. In the particular cases in which the equality happens at the minimum of the potential we have again stable circular orbits. Only in the case where $l=0$ particles can traverse the scalar star unaffected. For $m\neq 0$ there is still the possibility of finding a turning point, if the energy is low enough. However, if the particle is freely falling from infinity, with $E_\infty=1$, all energy is purely rest mass, it will radially traverse the star, as would do a photon.

We conclude that all orbits are not of the capture type. They can be circular, or unbound, and they all have at least one turning point. This helps to explain why a nonbaryonic object will not develop a singularity while still being a relativistic object [comparable effective potentials, equivalently, comparable relativisticity coefficient $GM(r)/r$].

V. GALACTIC PARAMETERS AND MASS

One interesting fact, which seems to be not referred before, is the point that for all these scalar stars, their radius is always related with the mass in the same way: $R\gtrsim Mm_{\rm Pl}^{-2}$.

This is indeed the statement—contrary to what it is usually assumed—that not all interesting astrophysical ranges of mass and radius can be modeled with scalar fields. In the scalar star models, from the given central mass, the radius we obtain for the star is comparable to that of the horizon $R \sim m_{\rm Pl}^{-2} \times 2.61 \times 10^6 M_\odot \sim 3.9 \times 10^{11}$ cm.

The question now is for which values of the parameters we can obtain a scalar object of such a huge mass. For the case of miniboson star we need an extremely light boson

$$m[\mathrm{GeV}] = 1.33 \times 10^{-25} \frac{M(\infty)}{M_{\rm BH}}. \tag{43}$$

Given a central density $\sigma(0)$, $M(\infty)$ stands for the dimensionless value of the boson star mass as seen by an observer at infinity. $M_{\rm BH}$ is the value of the black hole mass (in millions of solar masses), obtained by fitting observational data. Then, we are requiring that the total mass of the boson star equals that of the black hole. For instance, in Fig. 1, we have taken the data of Eckart and Genzel [41] and Genzel *et al.* [16], and fit them with a miniboson star with $\sigma(0) = 0.1$, which yields to a boson mass given by $m[\mathrm{GeV}] = 2.81 \times 10^{-26}$; the total mass of the star (without the cluster contribution) is 2.5×10^6 $\mathrm{M}_\odot$.

In the case of boson stars, and using the critical mass dependence, $\propto \sqrt{\lambda} m_{\rm Pl}^3 / m^2$, the requirement of a 2.5 million mass star yields to the following constraint:

$$m[\mathrm{GeV}] = 7.9 \times 10^{-4} \left(\frac{\lambda}{4\pi} \right)^{1/4}. \tag{44}$$

It is possible to fulfill the previous relationship, for instance, with a more heavy boson of about 1 MeV and $\lambda \sim 1$. A plot of this relation—for some values of λ—is shown in Fig. 9. Note that in this case, the value of the dimensionless parameter Λ is huge, and special numerical procedures, as explained above, must be used to obtain solutions. The characteristics of these solutions have proven to be totally similar to those with $\Lambda = 0$ which were used in Fig. 1, just the adimensionalization differs.

Finally, in the case of a nontopological soliton we obtain the following constraint,

$$m[\mathrm{GeV}] = \frac{7.6 \times 10^{12}}{\Phi_0^2 [\mathrm{GeV}]^2}. \tag{45}$$

For the usually assumed case, in which the order parameter Φ_0 is of equal value than the boson mass, we need very heavy bosons of unit mass $m = 1.2 \times 10^4$ GeV. Other possible pairs are shown in Fig. 10.

Boson candidates? Based on the constraints imposed by the mass-radius relationship valid for the scalar stars analyzed, we may conclude that (1) if the boson mass is comparable to the expected Higgs mass (hundreds of GeV), then the center of the galaxy could be a nontopological soliton star, (2) an intermediate mass boson could produce a superheavy object in the form of a boson star, and (3) for miniboson stars to be used as central objects for galaxies the existence of an ultralight boson is needed. These conclusions

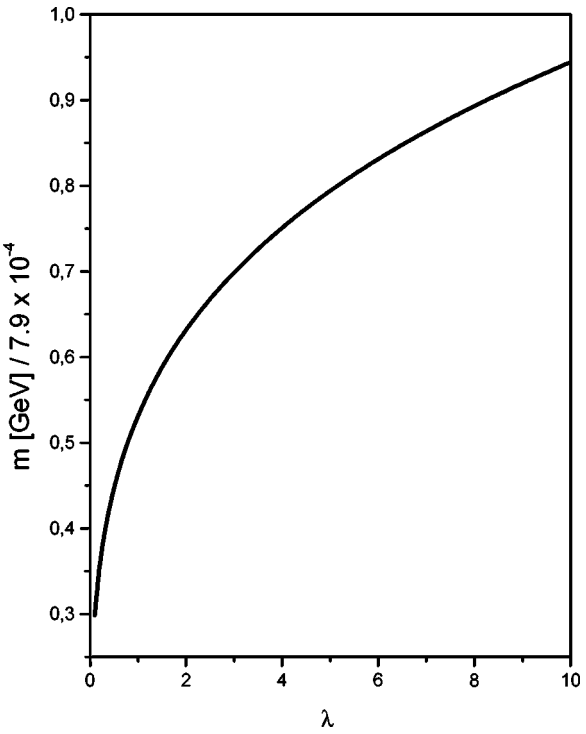

FIG. 9. Constraint in the boson star fundamental parameters which gives rise to an object of two million solar masses within approximately ten solar radius, consistent with the mass of the central object in our galaxy.

should be considered just as order of magnitude estimations. First, we are just considering (classical approach) static and uncharged stars, this is just a model (the simplest), but more complicated ones can exist. Secondly, we do not know the exact form of the self-interaction, or in the case of nontopological stars, the value of Φ_0. For instance, consider the Higgs boson mass. In the electroweak theory a Higgs boson doublet (Φ^+, Φ^0) and its antidoublet $(\Phi^-, \overline{\Phi}^0)$ are necessary ingredients in order to generate masses for the $W^\pm$ and Z^0 gauge vector bosons. Calculations of two-loop electroweak effects have led to an indirect determination of the Higgs boson mass [42]. For a top quark mass of $M_{\rm t} = 173.8 \pm 5$ GeV, the Higgs boson mass is $m_{\rm h} = 104^{+93}_{-49}$ GeV. However, experimental constraints are weak. The Fermilab Tevatron [43] has a mass range of $135 < m_{\rm h} < 186$ GeV, and together with the Large Hadron Collider (LHC) at CERN, they could decide if these Higgs particles (in the given range) exist in nature. Finally, a particle physics approach should be used in deciding if the needed self-interaction for each model is not in disagreement with renormalization properties.

We should also mention the possible dilatons appearing in low-energy unified theories, where the tensor field $g_{\mu\nu}$ of gravity is accompanied by one or several scalar fields. In string effective supergravity [44], for instance, the mass of the dilaton can be related to the supersymmetry breaking scale $m_{\rm SUSY}$ by $m_\varphi \simeq 10^{-3} (m_{\rm SUSY} / \mathrm{TeV})^2$ eV. Finally, a scalar with a long history as a dark matter candidate is the axion, which has an expected light mass $m_\sigma = 7.4 \times (10^7 \mathrm{\ GeV} / f_\sigma)$ eV $> 10^{-11}$ eV with decay constant f_σ

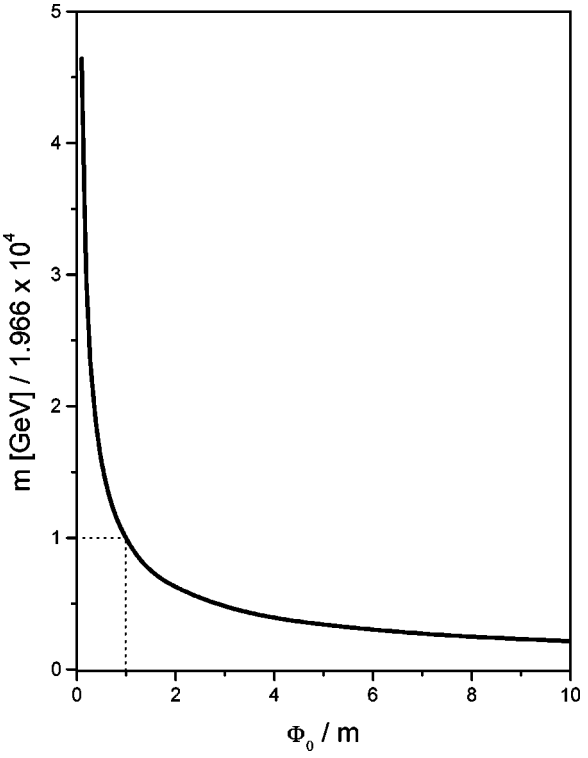

FIG. 10. Constraint in the nontopological soliton fundamental parameters which gives rise to an object consistent with the mass of the central object in our galaxy. It is specially marked for the usual case in which $\Phi = m$.

close to the inverse Planck time. Goldstone bosons have also inferred mass in the range of eV and less, $m_g < 0.06 - 0.3$ eV [45].

If boson stars really exist, they could be the remnants of first-order gravitational phase transitions and their mass should be ruled by the epoch when bosons decoupled from the cosmological background. The Higgs particle could be a natural candidate as constituent of a boson condensation if the phase transition occurred in early epochs. A boson condensation should be considered as a sort of topological defect relic. In this case, as we have seen, Sgr A* could be a soliton star. If soft phase-transitions took place during cosmological evolution (e.g., soft inflationary events), the leading particles could have been intermediate mass bosons and so our supermassive objects should be genuine boson stars. If the phase transitions are very recent, the ultralight bosons could belong to the Goldstone sector giving rise to miniboson stars. For the formation processes of boson stars the reader is referred to Refs. [33] and references therein. It is apparent that for every possible boson mass in the particle spectrum there is a boson star model able to fit the galactic center constraints, at least in order of magnitude.

VI. ACCRETION AND LUMINOSITY

A. Relativistic rotational velocities

For the static spherically symmetric metric considered here circular orbit geodesics obey

$$v_\varphi^2 = \frac{r\nu' e^\nu}{2} = e^\nu \frac{e^\mu - 1}{2} + \frac{8\pi}{m_{\rm Pl}^2} p_r r^2 \frac{e^{\mu+\nu}}{2} \simeq \frac{M(r)}{r} + \frac{8\pi}{m_{\rm Pl}^2} p_r r^2 \frac{e^{\mu+\nu}}{2}. \quad (46)$$

These curves increase up to a maximum followed by a Keplerian decrease. Schunck and Liddle [5] found that the possible rotation velocities circulating within the gravitational boson star potential are quite remarkable: their maximum reaches more than one-third of the velocity of light [5]. Schunck and Torres [6] proved that these high velocities are quite independent of the particular form of the self-interaction and are usually found in general models of boson stars. For instance, for $\Lambda = 0{,}300$ of the choice of Colpi *et al.* [29], $U_{\cosh} = \alpha m^2[\cosh(\beta\sqrt{|\psi|^2}) - 1]$, and $U_{\exp} = \alpha m^2[\exp(\beta^2|\psi|^2) - 1]$, the maximal velocities are 122 990 km/s at $x = 20.1$ for $\Lambda = 300$, 102 073 km/s at $x = 4.1$ for $\Lambda = 0$, 104 685 km/s at $x = 4.2$ for $U_{\exp}$, and 102 459 km/s at $x = 5.9$ for $U_{\cosh}$ [6].

With such high velocities, the matter possesses an impressive kinetic energy, of about 6% of the rest mass; i.e., to obtain the required luminosity we would need that about 10^{-8} to 10^{-7} solar masses per year be transformed into radiation. Note that the required matter-radiation transfer is at least two orders of magnitude smaller than the accretion rate towards Sgr A*.

The maximum rotational speed is attained well outside the physical radius of the star, as can be seen by computing the dimensionless x value for the star radius (e.g., it happens between $x \sim 5$ and 15 for Λ going from 0 to 300). It is interesting to note also that the dependence of the maximum velocity on Λ is not very critical, and the same process can be operative with miniboson stars. The rotational velocity is dependent on the central density, increasing with a higher value of σ_0. To obtain large rotational velocities, it is needed that the central density of the star be highly relativistic, for Newtonian solutions velocities are low and quite constant over a larger interval. This is consistent with the density constraint of the dark object in Sgr A*.

B. The (baryonic) black hole danger

How can one justify that the accretion onto the central object—a neutrino ball or a boson star—will not create a black hole in its center anyway. Interstellar gas and stars, while spiraling down towards the center of the object, will collide with each other, and may glue together at the center, what could be the seed for a very massive black hole. Even a black hole of small mass can spiral inwards, and if it remains at the center, that black hole itself could be the seed. On the other hand, stellar formation of massive stars would yield, after evolution, to a black hole. Then, we need to consider whether there is a mechanism that prevents the formation of a very massive baryonic object—leading inevitably to a black hole—in the center of the galaxy.

The key aspect to consider is disruption. A star interacting with a massive object cannot be treated as a point mass when

it is close enough to the object such that it becomes vulnerable to tidal forces. Such effects become important when the pericentre $r_{\min}$ is comparable to the tidal radius [46]

$$r_t = 5\times 10^{12} M_6^{1/3}\left(\frac{R_*}{R_\odot}\right)\left(\frac{M_*}{M_\odot}\right)^{-1/3} \text{ cm}. \tag{47}$$

Here, $R_{*,\odot}$ stands for the radius of the star and the sun respectively, while $M_{*,\odot}$ for the masses. M_6 is the mass of the central object in millions of solar masses. r_t is the distance from the center object at which M/r^3 equals the mean internal energy of the passing star. Only for black holes with masses smaller than $10^8 M_\odot$ and for certain low density stars—red giants—we can expect that the disruption happens outside the event horizon. This is the reason why supplying the material at lower densities, with the black hole gravity dominating the situation, can generate more power. Rees [46] has also given an estimate of how frequently a star enters this zone. When star velocities are isotropic, the frequency with which a solarlike star passes within a distance $r_{\min}$ is

$$\sim 10^{-4} M_6^{4/3}\left(\frac{N_*}{10^5 \ \text{pc}^{-3}}\right)\left(\frac{\sigma}{100 \ \text{km s}^{-1}}\right)\left(\frac{r_{\min}}{r_t}\right)\text{yr}^{-1}, \tag{48}$$

where N_* is the star density and σ the velocity distribution. Disruptions are rare events that happen once in about 10 000 yrs.

Because of the similar metric potentials, far from the center of the nonbaryonic star, the accretion mechanism will be the same as that operative in the Schwarzschild case. If a boson star is in the center of the galaxy, the characteristics of the tidal radius and the time scale of disruption occurrence will be similar to those of a black hole of equal mass. However, stars falling inwards will *all* be disrupted after they approach a minimum radius. Contrary to black holes of big masses, which can swallow stars as a whole and disrupt them behind their event horizons, boson stars will disrupt all stars—most stars outside and a few inside the Schwarzschild radius of a black hole of equal mass—at everyone's sight.

In the case of black holes, the most recent simulations [47] show that up to 75% of the mass that once formed the disrupted star become unbound. For boson stars, we argue that once the star is disrupted to test particles (with masses absolutely negligible to that of the central object), and because there are no capture orbits (see Figs. 7 and 8), all particles follow unbound trajectories. All material is diverted from the center and the formation of a black hole is avoided.

It would be worthwhile to perform numerical simulations changing the central object from a black hole to a boson star, to see the aftermath and the fate of the debris in an actual boson-star-generated disruption. This, however, could well not be an easy task: In black hole simulations, the minimum radius is maintained still far from the center ($\sim$10 Schwarzschild radius), where Newtonian or Post-Newtonian approximations are valid. To actually see the difference between a black hole and a boson star it could be necessary to attain inner values of radii, where the behavior is completely relativistic.

One case could merit further attention: the possible spiraling of a black hole of stellar size. This case may complicate the situation since a black hole cannot be disrupted. However, differences in masses are so large that it will behave as a test particle for the boson central potential, and also will be diverted from the center. Moreover, being of stellar size, it will be appreciably influenced by other intruding stars, also making it be left in a static position at the boson star center.

C. Any nonbaryonic danger?

One may as well ask if a continuous inflow of nonbaryonic particles may affect the central object. Let us suppose that the inflow of bosons has the same accretion rate as normal matter. This may indeed be seen as an upper bound, since a large inflow of nonbaryonic mass would affect the accretion disk gravitationally. In the lifetime of the universe, the accreted nonbaryonic mass would be at least two orders of magnitude smaller than the mass of the boson star itself. Then, if we consider that this process makes the star to evolve in an adiabatical series of equilibrium states, only boson stars with central density extremely close to the critical value could be affected by the evolution. Since we may construct models in a large range of central densities, this appears to present no problem for the object to survive.

A detailed analysis of the evolution of boson stars subject to continuos inflow of nonbaryonic particles was carried out by Seidel and Suen [48]. Their results showed that under finite (noninfinitesimal) perturbations, with possible changes in the mass and the number of boson present in the configuration, such as the accretion phenomenon, the configurations on the stable branch, when perturbed, will oscillate, emit scalar field radiation and settle down into a new configuration with less mass and a larger radius. Then, the accretion of nonbaryonic matter (possibly entering into the condensate through gravity forces and scattering from the outer parts of the halo) seems not to present an issue for these kinds of models.

D. Comments on neutrino balls

If the center of the galaxy is a neutrino ball, one also has to obtain a mechanism that prevents the formation of a very massive baryonic object. However, caused by the fact that a neutrino ball is an extended object and that the gravitational potential is shallower, we have to expect very crucial differences with a boson star case. The first thing to note is that r_t is well within the neutrino ball, and then, stars will traverse the exterior parts of the ball without being disrupted. In doing so, however, the central mass that they see at the center will be less than the total mass of the ball, and at a distance $r = r_t$ the mass enclosed is negligible. Disruption cannot proceed. We note then that the observation of a disruption in the center of a galaxy is then indicative that a neutrino ball is not there.

When the mass enclosed by the neutrino ball is small enough [say, $\mathcal{O}(10^3)M_\odot$], the accretion disk will be unstable. This happens about 0.1 – 1 light yr from the center. There, stars which could actually form at a rate of 1 per hundred thousand years (the actual number will depend on the mass of the star) will be probably kicked off by intruding stars [49,50]. The absence of the disruption mechanism makes this problem worse, since given an enough amount of time, it is hard to think of compelling reasons by which gas and stars are expelled from the center. To us, it is yet an unclear issue in the neutrino ball scenario.

VII. DISCUSSION: HOW TO DIFFERENTIATE BETWEEN A SUPERMASSIVE BLACK HOLE AND A BOSON STAR?

One of the easiest things one may think of is to follow the trajectory of a particular star. The trajectory of S1, for instance, a fast moving star near Sgr A*, offers the possibility of distinguishing between a black hole and a neutrino condensate, since Newtonian orbits deviate from each other by several degrees in a period of some years [51]. However, as soon as the central object is not so extended, as in the boson star case, this technique is useless (in every case in which the pericenter is further than the tidal radius), and other forms of detecting their possible presence have to be devised.

The second possibility is to make an in-depth study of the properties of the accretion disk. This gets complicated by the fact that the metric of boson stars is not analytically known. However, preliminary studies in the case of the simplest—black body behaving—accretion disk have shown that the spectrum of the radiation emitted is modified, especially at high energies [52]. To directly compare with data on Sgr A* we would need to develop more advanced models of the accretion disk.

It has been already noted that x-ray astronomy can probe regions very close to the Schwarzschild radius. Recent results from the Japanese-U.S. ASCA mission have revealed broadened iron lines, a feature that comes from regions which are under strong gravitational influence. In particular, Iwasawa *et al.* claimed that ASCA observations to Seyfert 1 galaxy MCG-6-30-15 got data from 1.5 gravitational radii, and conclude that the peculiar line profile suggests that the line-emitting region is very close to a central spinning (Kerr) black hole where enormous gravitational effects operate. By the way, this is stating that a neutrino ball cannot be the center of that galaxy, since its gravitational potential is shallow. However, as was already noted [5], a boson star could well be a possible alternative, and x rays could be used to map out in detail the form of the potential well. The NASA Constellation-*X* [53] mission, to be launched in 2008, is optimized to study the iron *K* line feature discovered by ASCA and, if they are there, will determine the black hole mass and spin for a large number of systems. Still, Constellation-*X* will provide an indirect measure of the properties of the region within a few event horizon radii. A definite answer in this sense will probably be given by NASA-planned MAXIM mission [54], a μ-arcsec *X*-ray imaging mission, that would be able to take direct *X*-ray pictures of regions of the size of a black hole event horizon. Both of these space missions will have the ability to give us proofs of black hole existence, or to provide evidence for more strange objects, such as boson stars.

Very recently, Falcke *et al.* [55] have noted that observations of very large baseline interferometry (VLBI) could give the signature to discriminate among these models. Falcke *et al.* assumed that the overall specific intensity observed at infinity is an integration of the emissivity (taken as independent of the frequency or falling as r^{-2}) times the path length along geodesics. Defining the apparent boundary of a black hole as the curve on the sky plane which divides a region where geodesics intersects the horizon from a region whose geodesics miss the horizon, they noted that photons on geodesics located within the apparent boundary that can still escape to the observer will experience strong gravitational redshift and a shorter total path length, leading to a smaller integrated emissivity. On the contrary, photons just outside the apparent boundary could orbit the black hole near the circular photon radius several times, adding to the observed intensity. This is what produces a marked deficit of the observed intensity inside the apparent boundary, which they refer to as the ''shadow'' of the black hole. The apparent boundary of the black hole is a circle of radius $27R_g$ in the Schwarzschild case, which is much larger than the event horizon due to strong bending of light by the black hole. This size is enough to consider the imaging of it as a feasible experiment for the next generation of mm and sub-mm VLBI. While the observation of this shadow would confirm the presence of a single relativistic object, a nondetection would be a major problem for the current black hole paradigm.

In the case of a boson star, we might expect some diminishing of the intensity right in the center, this would be provided by the effect on relativistic orbits, however, this will not be as pronounced as if a black hole is present: for that case, many photons are really gone through the horizon and this deficit also shows up in the middle. If a boson star is there, some photons will traverse it radially, and the center region will not be as dark as in the black hole case. A careful analysis of Falcke *et al.*'s shadow behavior replacing the central black hole with a boson star model would be necessary to get any further detail, and eventually an observable prediction.

We also mention that the project ARISE (Advanced Radio Interferometry between Space and Earth) is going to use the technique of Space VLBI to increase our understanding of black holes and their environments. The mission, to be launched in 2008, will be based on a 25-m inflatable space radio telescope working between 8 and 86 GHz [56]. It will study gravitational lenses at resolutions of tens of μ arcsecs, yielding information on the possible existence (and signatures) of compact objects with masses between $10^3M_\odot$ and $10^6M_\odot$.

Another technique for detecting boson stars from other relativistic objects will be gravitational wave measurements [57]. If a particle with stellar mass is observed to spiral into a spinning object with a much larger mass and a radius comparable to its Schwarzschild length, from the emitted gravi-

tational waves, one could obtain the lowest multipole moments. The black hole no-hair (or two-hair) theorem establishes that all moments are determined by its lowest two, the mass and angular momentum (assuming that the charge equals zero), for instance, the mass quadrupole moment would give $M_2=-L^2/M$. Should this not be so, the central object would not be a black hole, and as far as we know, the only remaining viable candidate would be a boson star. In this case, Ryan [57] have proven a sort of three-hair theorem (in general relativity) such that all multipole moments are determined by the boson stars lowest three. Even more, he has shown that given these lowest three moments we shall be able to determine the free parameters in the Lagrangian (the mass of the boson particle and the self-interaction). If these parameters provide an object of the size and mass of a galactic center, then the case for nonbaryonic objects at the nuclei of galaxies would be proven. In ten years time, a combination of gravitational wave measurements, better determination of stellar motions, and mm and sub-mm VLBI techniques could give us a definite picture of the single object at the center of our Milky Way, as well at the center of other galaxies.

VIII. CONCLUSIONS

We have shown that boson and soliton stars provide (for a large range of boson masses and self-interactions) the basic necessary ingredients to fit dynamical data and observed luminosity of the center of the Galaxy. They appear to constitute viable alternatives for the central supermassive object, producing a theoretical curve for the projected stellar velocity dispersion consistent with Keplerian motion, relativistic rotational velocities, and having an extremely small size. The fact that boson stars do not have a solid surface avoids the emission of big amounts of x rays—generated by collisions—something which is in agreement with observations. Much work has yet to be done to analyze in detail the physics of the accretion disk around a supermassive boson star, but we have commented that we are already on the verge of having the right tools to discriminate the presence, or the absence, of horizons in galactic nuclei.

Other singularity-free models were considered as well, such as, e.g., neutrino or gravitino condensations. In this case, the object is sustained by its Fermi energy, while in the boson star case, it is the Heisenberg's Uncertainty Principle which prevents the system from collapsing to a singularity. Due to this fact, boson stars are genuine relativistic objects where a strong gravitational field regime holds. The difference in the relativistic status of both objects is not trivial. While fermion neutrino balls are extended objects, boson stars mimic a black hole. Disruption processes cannot happen in a fermion condensation, and it has the unpleasant consequence of not providing with a straightforward mechanism by which stars could be diverted from the center, and through which finally avoid the formation of a massive black hole inside the condensate.

The formation of boson stars and black holes can be competitive processes. Then, it might well be that even if we discover that a black hole is in the center of the galaxy, others galaxies could harbor nonbaryonic centers. In the case of boson stars, only after the discovery of the boson mass spectrum we shall be in position to determine *a priori* which galaxies could be modeled by such a center. Observations of galactic centers could then suggest the existence of boson scalars much earlier than their discovery in particle physicists labs.

ACKNOWLEDGMENTS

We acknowledge insightful comments by H. Falcke, S. Guzmán, F. Schunck, I. Tkachev, D. Tsiklauri, L. Urena-Lopez, R. Viollier, and A. Whinnett. Also, we acknowledge informal talks with D. Bennet, R. di Stefano, C. Kochanek, and A. Zaharov at the Moriond 2000 meeting, and with E. Mielke and A. Iwazaki at the Marcel Grossman Meeting. D.F.T. was supported by CONICET as well as by funds granted by Fundación Antorchas, and we particularly thank G. E. Romero for his encouragement and criticism, and the ICTP and the University of Salerno (Italy) for hospitality. S.C. and G.L.'s research was supported by MURST fund (40%) and art. 65 D.P.R. 382/80 (60%). G.L. further thanks UE (P.O.M. 1994/1999).

APPENDIX

For the reader's convenience, we quote here the dimensional conversion for the radius and the mass of a boson star. Using the value of 1 GeV in cm^{-1}, and taking into account the dimensionless parameter $x=mr$, we get

$$r[\mathrm{pc}]=\frac{x}{m[\mathrm{GeV}]}6.38\times10^{-33}. \tag{A1}$$

For the mass, recalling that $M=M(x)m_{\mathrm{Pl}}^2/m$, we get

$$M[10^6M_\odot]=\frac{M(x)}{m[\mathrm{GeV}]}1.33\times10^{-25}. \tag{A2}$$

In the case where $\Lambda\gg1$, both right hand sides of the previous formulas get multiplied by $\Lambda^{1/2}$.

[1] T. Matos, F. S. Guzmán, and L. A. Urena-Lopez, Class. Quantum Grav. **17**, 1707 (2000); F. S. Guzmán and T. Matos, *ibid.* **17**, L9 (2000); T. Matos, F. S. Guzmán, and D. Núñez, Phys. Rev. D **62**, 061301 (2000).
[2] A. Riotto and I. Tkachev, Phys. Lett. B **484**, 177 (2000).
[3] S. Perlmutter *et al.*, Astrophys. J. **517**, 565 (1999).
[4] M. Célérier, Astron. Astrophys. **353**, 63 (2000).
[5] F. E. Schunck and A. R. Liddle, Phys. Lett. B **404**, 25 (1997).
[6] F. E. Schunck and D. F. Torres, Int. J. Mod. Phys. D (to be published), gr-qc/9911038.
[7] S. Capozziello, G. Lambiase, and D. F. Torres, Class. Quantum Grav. **17**, 3171 (2000).

[8] I. Tkachev, Sov. Astron. Lett. **12**, 305 (1986); Phys. Lett. B **191**, 41 (1987); **261**, 289 (1991).
[9] A. Iwazaki, Phys. Lett. B **455**, 192 (1999).
[10] M. P. Dabrowski and F. E. Schunck, Astrophys. J. (to be published), astro-ph/9807207.
[11] K. S. Virbhadra, D. Narasimha, and S. M. Chitre, Astron. Astrophys. **337**, 1 (1998).
[12] K. S. Virbhadra and G. F. R. Ellis, astro-ph/9904193, 1999.
[13] D. F. Torres, G. E. Romero, and L. A. Anchordoqui, Phys. Rev. D **58**, 123001 (1998); Mod. Phys. Lett. A **13**, 1575 (1998).
[14] R. Genzel, D. Hollenbach, and C. H. Townes, Rep. Prog. Phys. **57**, 417 (1994).
[15] A. M. Ghez, B. L. Klein, M. Morris, and E. E. Becklin, Astrophys. J. **509**, 678 (1998).
[16] R. Genzel, N. Thatte, A. Krabbe, H. Kroker, and L. E. Tacconi-Garman, Astrophys. J. **472**, 153 (1996).
[17] R. H. Sanders, Nature (London) **359**, 131 (1992).
[18] E. Maoz, Astrophys. J. Lett. **447**, 91 (1995).
[19] H. C. Ford *et al.*, Astrophys. J. Lett. **435**, 27 (1994).
[20] D. Macchetto *et al.*, Astrophys. J. **489**, 579 (1997).
[21] L. J. Greenhill, D. R. Jiang, J. M. Moran, M. J. Reid, K. Y. Lo, and M. J. Claussen, Astrophys. J. **440**, 619 (1995).
[22] J. Kormendy and D. Richstone, Annu. Rev. Astron. Astrophys. **33**, 581 (1995).
[23] H. Falcke and O. M. Heinrich, Astron. Astrophys. **292**, 430 (1994).
[24] D. Tsiklauri and R. D. Viollier, Astrophys. J. **500**, 591 (1998).
[25] S. Capozziello and G. Iovane, Phys. Lett. A **259**, 185 (1999).
[26] J. H. Krolik, *Active Galactic Nuclei* (Princeton University Press, Princeton, NJ, 1999).
[27] M. Miyoshi *et al.*, Nature (London) **373**, 127 (1995).
[28] J. J. Binney and S. C. Tremaine, *Galactic Dynamics* (Princeton University Press, Princeton, NJ, 1987).
[29] M. Colpi, S. L. Shapiro, and I. Wasserman, Phys. Rev. Lett. **57**, 2485 (1986).
[30] T. D. Lee, Phys. Rev. D **35**, 3637 (1987); R. Friedberg, T. D. Lee, and Y. Pang, *ibid.* **35**, 3640 (1987); **35**, 3658 (1987); **35**, 3678 (1987).
[31] D. J. Kaup, Phys. Rev. **172**, 1331 (1968).
[32] R. Ruffini and S. Bonazzola, Phys. Rev. **187**, 1767 (1969).
[33] T. D. Lee and Y. Pang, Phys. Rep. **221**, 251 (1992); A. R. Liddle and M. S. Madsen, Int. J. Mod. Phys. D **1**, 101 (1992); E. W. Mielke and F. E. Schunck, in *Proceedings of the 8th Marcel Grossmann Meeting*, Jerusalem, Israel (World Scientific, Singapore, 1999), gr-qc/9801063.
[34] F. V. Kusmartsev, E. W. Mielke, and F. E. Schunck, Phys. Rev. D **43**, 3895 (1991); Phys. Lett. A **157**, 465 (1991).
[35] R. C. Tolman, *Relativity, Thermodynamics and Cosmology* (Oxford, Clarendon, 1934).
[36] D. F. Torres, Phys. Rev. D **56**, 3478 (1997); D. F. Torres, A. R. Liddle, and F. E. Schunck, *ibid.* **57**, 4821 (1998); D. F. Torres, F. E. Schunck, and A. R. Liddle, Class. Quantum Grav. **15**, 3701 (1998); G. L. Comer and H. Shinkai, *ibid.* **15**, 669 (1998); A. W. Whinnett and D. F. Torres, Phys. Rev. D **60**, 104050 (1999); A. W. Whinnett, *ibid.* **61**, 124014 (2000).
[37] F. E. Schunck and E. W. Mielke, in *Proceedings of the Bad Honnef Workshop, Relativity and Scientific Computing: Computer Algebra, Numerics, Visualization*, edited by F. W. Hehl, R. A. Puntigam, and H. Ruder (Springer-Verlag, Berlin, 1996), pp. 8 and 138; S. Yoshida and Y. Eriguchi, Phys. Rev. D **56**, 762 (1997).
[38] Ph. Jetzer and J. J. van der Bij, Phys. Lett. B **227**, 341 (1989).
[39] B. Punsly, Astrophys. J. **498**, 640 (1998); B. Punsly, G. E. Romero, D. F. Torres, and J. Combi, astro-ph/0007465, 2000.
[40] S. L. Shapiro and S. A. Teukolsky, *Black Holes, White Dwarfs and Neutron Stars* (Wiley, New York, 1983), p. 350.
[41] A. Eckart and R. Genzel, Nature (London) **383**, 415 (1996); Mon. Not. R. Astron. Soc. **284**, 576 (1997).
[42] P. Gambino, talk given in RADCORE 98, International Symposium on Radiative Corrections, Barcelona, 1998.
[43] T. Han and R. J. Zhang, Phys. Rev. Lett. **82**, 25 (1999).
[44] S. Ferrara, C. Kounnas, and F. Zwirner, Nucl. Phys. **B429**, 589 (1994); **B433**, 255(E) (1995).
[45] H. Umeda, N. Iwamoto, S. Tsuruta, L. Qin, and K. Nomoto, in *Proceedings of the Symposium Neutron Stars and Pulsars*, edited by N. Shibazaki (World Scientific, Singapore, 1998), p. 213.
[46] M. D. Rees, Nature (London) **333**, 523 (1988).
[47] S. Ayal, M. Livio, and T. Piran, astro-ph/0002499, 2000.
[48] E. Seidel and W. Suen, Phys. Rev. D **42**, 384 (1990).
[49] R. D. Viollier (private communication).
[50] D. Tsiklauri and R. D. Viollier, Astropart. Phys. **122**, 199 (1999).
[51] F. Munyaneza, D. Tsiklauri, and R. D. Viollier, Astrophys. J. Lett. **509**, 105 (2000).
[52] D. F. Torres (in preparation).
[53] Constellation *X* satellite web page: URL http://constellation.gsfc.nasa.gov/
[54] Maxim satellite web page: URL http://maxim.gsfc.nasa.gov/
[55] H. Falcke, F. Melia, and E. Agol, Astrophys. J. Lett. **528**, 13 (2000).
[56] J. S. Ulvestad, astro-ph/9901374, 1999.
[57] F. Ryan, Phys. Rev. D **55**, 6081 (1997).